Analysis of the Failure of Ceramics Due to Subcritical Crack Growth

François Hild, Didier Marquis, Olivier Kadouch, Jean-Pierre Lambelin

François Hild
Chargé de Recherche au C.N.R.S.

Didier Marquis
Professor.

*Laboratoire de Mécanique et Technologie,
E.N.S. Cachan/C.N.R.S./Université Paris 6,
61, avenue du Président Wilson,
F-94235 Cachan Cedex, France

Olivier Kadouch
Research Scientist,
Commissariat à l'Energie Atomique,
Centre d'Etudes de Vaujours-Moronvilliers,
B.P. No 7, F-77181 Courtry, France

Jean-Pierre Lambelin
Research Scientist,
Commissariat à l'Energie Atomique,
Centre d'Etudes du C.E.S.T.A., B.P. No 2,
F-33114 Le Barp, France

Analysis of the Failure of Ceramics Due to Subcritical Crack Growth

Failure conditions are assessed when ceramics exhibit Subcritical Crack Growth from preexisting flaws. In the framework of the weakest link theory and independent events hypothesis, a reliability analysis is carried out by modeling flaw distributions and crack growth laws. Experimental data obtained on a spinel Mn Zn ferrite subjected to five different load rates are analyzed by using an expression for the failure probability accounting for Subcritical Crack Growth.

1 Introduction

The need for high performance materials has motivated the use of structures made of brittle materials. Such materials are usually characterized by a large scatter in strength leading to a requirement for a statistical treatment of strength properties. For design purposes, a statistical failure analysis should allow the use of experimental data obtained on small specimens subjected to simple load patterns, to infer the failure probability of structures under complex stress states encountered in service.

It is now well accepted that initial flaws cause catastrophic failure by fracture of structures made of ceramics. These initial flaws are usually randomly distributed, and lead to different strengths, even though the geometry and the loading conditions are identical. The failure condition is given by the probability of finding one critical flaw within a structure. To be critical, a flaw needs to be large enough and located in a sufficiently high loaded region. This critical flaw then represents "the weakest link" of the structure.

To predict failure conditions, various expressions of the failure probability have been proposed. Generally, they are deduced from both the weakest link theory and the independent events hypothesis. The first attempt was made by Weibull (1939), and was based upon an empirical treatment of failure. Yet "this approach does not recognize the flaws as being unique entities operated on by the multiaxial stress and does not, therefore, represent a fundamental way of treating the multiaxial effect (Evans, 1978)." Batdorf and Crose (1974) modeled initial flaws by cracks whose size and orientation are randomly distributed. Evans and Lamon (1978; 1983; 1988) derived another model based upon similar assumptions. The drawback of these approaches is that they are not easily extendable to cases where the material behavior is time-dependent, i.e., exhibiting Subcritical Crack Growth.

In the framework of Linear Elastic Fracture Mechanics, Jayatilaka and Trustrum (1977) showed that under some simplifying assumptions the Weibull parameters can be related to flaw distributions. These results have been extended in the framework of Linear Elastic Fracture Mechanics and Continuum Damage Mechanics (Hild and Marquis, 1992). An expression for the failure probability was obtained, in which the flaw distribution was directly considered. Therefore, when the material is exhibiting Subcritical (or Slow) Crack Growth (SCG), the initial flaw distribution evolves with time, and the previous approach can still be used. Some attempts have been made by Aoki et al. (1980; 1983) but by assuming that the time effects can be decoupled from the stress effects. This assumption is generally not valid: Hild and Roux (1991) obtained an expression for the flaw size distribution after a time t related to the initial flaw size distribution (i.e., $t = 0$). More recent results can be found in (Brinkman and Duffy, 1994); most of the approaches do not explicitly consider the flaw distribution. The aim of this paper is to derive an expression for the failure probability taking account of the evolution of the flaw distribution for materials with a time-dependent behavior.

Section 2 is devoted to deriving an expression for the failure probability of a structure made of a material with a time-dependent behavior. This expression is derived within the framework of the weakest link theory and the independent events hypothesis. It consists in modeling the mechanical behavior of a single link and studying the failure of a structure composed of several links. In Section 3 the general equations governing Subcritical Crack Growth are presented. Approximations are made in order to derive tractable expressions. Based upon the hypotheses of Section 3, Section 4 deals with a simplified expression for the failure probability of a structure made of a material with a time-dependent behavior. The failure probability of a single link is related to an initial flaw size distribution. To assess the reliability of a Representative Volume Element (RVE), one needs to calculate the initial critical flaw size under static and dynamic conditions. An upper bound and a lower bound of the failure probability are then derived. In Section 5, the previous results are studied when the flaw size distribution is modeled by a modified Gamma function. In particular, a Weibull law can be derived by using simplifying assumptions. Lastly, in Section 6, experimental data obtained on a spinel Mn Zn ferrite are compared with predictions using the previous results.

2 Reliability of Structures Containing Flaws With a Time-Dependent Failure Behavior

In general, initial flaws are randomly distributed within a structure. We assume that the flaw distribution is characterized by a probability density function f. The function f gives the flaw distribution at a given stage of the load history. The function f may depend upon several morphological parameters w (e.g., a flaw size denoted by a; a flaw direction characterized by a normal $\underline{n}$).

2.1 Failure Probability of a Representative Volume Element. The failure probability, P_{F0}, of an RVE is given by the probability of finding a critical flaw within an element Ω_0 of volume V_0. The probability of finding a critical flaw refers to the *initial* flaw distribution characterized by a probability density function f_0. For a given load level, the set of flaws $\mathcal{D}$ splits into two subsets. The first subset, $\mathcal{D}_c$, is related to the flaws that are critical (e.g., the energy release rate $\mathcal{G}(w, Q) \geq \mathcal{G}_c$, where Q is a loading parameter, and $\mathcal{G}_c$ a critical energy release rate). The second one, $\mathcal{D}_{nc}$, is related to the flaws that are not critical (e.g., $\mathcal{G}(w; Q) < \mathcal{G}_c$). The higher the load level, the larger $\mathcal{D}_c$ becomes with respect to $\mathcal{D}_{nc}$. The determination of the critical flaws depends upon the mechanical modeling of the flaw (Hild and Marquis, 1992). Some particular expressions can be found in the literature: Weibull (1939) used the "mode I" energy release rate, Batdorf and Crose (1974) used the coplanar energy release rate, Lamon and Evans (1983) used the non-coplanar energy release rate. When propagation is unstable, the failure probability $P_{F0}(Q)$ of a volume Ω_0 for a given loading parameter Q is given by

$$P_{F0}(Q) = \int_{\mathcal{D}_c(Q)} f_0(w)dw \tag{1}$$

with, for instance, $\mathcal{D}_c(Q) = \{w | \mathcal{G}(w; Q) \geq \mathcal{G}_c\}$. In the case of stable propagation, the initial morphological parameters w evolve to become W after an instant τ. In particular, bifurcation may take place (therefore $\underline{N} \neq \underline{n}$, and other morphological parameters may be needed). The morphological parameters W are assumed to be uniquely related to their initial values w through deterministic functions of C^1 class

$$W = \xi(w; Q, \tau) \tag{2}$$

At an instant τ and a fixed Q, the failure probability $P_{F0}(Q, \tau)$ is linked with the flaw density function f_τ

$$P_{F0}(Q, \tau) = \int_{\mathcal{D}_c(Q)} f_\tau(W; Q, \tau)dW \tag{3}$$

e.g., $\mathcal{D}_c(Q) = \{W | \mathcal{G}(W; Q) \geq \mathcal{G}_c\}$. If no new cracks initiate during the loading, f_τ is related to f_0 by (Hild and Marquis, 1995)

$$f_\tau[\xi(w; Q, \tau)] = J^{-1}(w; Q, \tau) f_0(w) \tag{4}$$

where J denotes the Jacobian of the transformation defined in Eq. (2). This relationship is a generalization of the results derived in the case of a flaw size distribution (Hild and Roux, 1991). Through Eq. (4), Eq. (3) can be written as Eq. (5), where $\mathcal{D}_c^*$ defines the initial flaws that become critical after τ

$$P_{F0}(Q, \tau) = \int_{\mathcal{D}_c^*(Q,\tau)} f_0(w)dw \tag{5}$$

e.g., $\mathcal{D}_c^*(Q, \tau) = \{w | \mathcal{G}[\xi(w; Q, \tau); Q] \geq \mathcal{G}_c\}$. Equation (5) constitutes a unified expression for the failure probability with or without SCG. It relates the failure probability to the initial flaw distribution f_0.

2.2 Failure Probability of a Structure Under Time-Dependent Conditions. If we assume that the interaction between flaws is negligible, the expression for the failure probability, P_F, of a structure Ω of volume V can be derived in the framework of the weakest link theory and with the independent events assumption. When the material behavior is either time-dependent or time-independent, the expression for P_F can be related to the failure probability, P_{F0}, of a link by (Freudenthal, 1968)

$$P_F = 1 - \exp\left\{\frac{1}{V_0}\int_\Omega \ln(1 - P_{F0})dV\right\} \tag{6}$$

The failure probability, P_{F0}, as well as the failure probability, P_F is a function of the loading parameter Q and elapsed time τ. By means of Eqs. (5) and (6), a general relationship between the initial flaw distribution and the failure probability of a structure Ω can be derived

$$P_F(Q, \tau) = 1 - \exp\left\{\frac{1}{V_0}\int_\Omega \ln\left(1 - \int_{\mathcal{D}_c^*(Q,\tau)} f_0(w)dw\right)dV\right\} \tag{7}$$

Equation (7) constitutes the main result of this section. The failure probability of a structure can be related to the initial flaw distribution even for materials exhibiting time-dependent behaviors. The time dependence is given in the definition of the set of initial defects that become critical after an instant τ and when the applied load level is equal to Q. Equation (7) constitutes a generalization of the existing failure probabilities only valid under time-independent behavior. It is worth noting that Eq. (7) allows the competition of flaws of different sizes at different locations with different stress levels, and the weakest link is not necessarily a flaw located at the most loaded point(s) but the most critical flaw defined by $\mathcal{G}[\xi(w; Q, \tau); Q] \geq \mathcal{G}_c$.

3 Modeling of Subcritical Crack Growth

In this section, the evolution law of a single flaw is analyzed. The aim of this section is to study different expressions of Eq. (2) obtained experimentally.

3.1 Crack Propagation Under Pure Mode I Conditions. Brittle fracture of ceramic materials is often preceded by SCG. This behavior leads to a time-dependence of the failure strength (Evans, 1972; Evans and Wiederhorn, 1974). This effect is due to the interaction between the environment and the material. A sensitivity of a ceramic to SCG is measured by the evolution of mode I stress intensity factor K versus crack growth rate da/dt. Usually, the $K - da/dt$ curve is schematically described by the curve given in Fig. 1 (Evans, 1972). Region I corresponds to somewhat low stress levels. The chemical reaction at the crack tip controls the crack propagation. Evans and Wiederhorn (1974) proposed to model this region by the following relationship

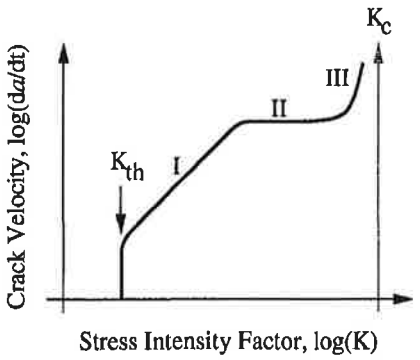

Fig. 1 Schematic representation of the effect of stress intensity factor, K, on crack velocity, da/dt, during Subcritical Crack Growth.

$$\frac{da}{dt} = CK^n,\ K \geq K_{th} \tag{8}$$

where C, n are material parameters, and a the flaw size. The parameter n can be used as a measure of material sensitivity to SCG: the higher n, the lower the sensitivity to SCG. Region I is characterized by a threshold stress intensity factor K_{th} (or a threshold energy release rate $\mathcal{G}_{th}$) under which no growth occurs. For example, the spinel Mn Zn ferrite exhibits SCG when double torsion experiments are performed in air at room temperature. The value of the parameter n is found equal to 20 (Kadouch, 1993). Region II corresponds to the diffusion of corrosive species to the crack tip. This diffusion controls the crack growth. The characteristic of the region is a constant velocity. Region III sometimes exits. Yet, the crack velocities are very high in the two last regions as compared to the first region. The fracture condition given by $\mathcal{G} \geq \mathcal{G}_c$ can be rewritten in terms of stress intensity factors under a pure mode I loading condition $K = K_c$. Equation (8) agrees with most of the experimental data for ceramics exhibiting SCG. These data were established on macrocracks under pure mode I, and therefore they did not experience kinking. Under mixed mode conditions however, kinking may take place and the previous laws may not be applicable anymore.

3.2 General Case and Approximations. In practice, most of the intrinsic flaws observed in ceramics are either cavities or inclusions of hard materials (Kingery et al., 1976). The most likely shape can be approximated by a sphere of radius a. Initiation is assumed to occur in a plane perpendicular to the direction of maximum principal stress, σ_1, and the initial flaw is assumed to be penny shaped. If the load history is simple (i.e., the direction of principal stresses does not change), then micro propagation happens in the same plane as micro initiation and no kinking is involved (Bilby and Cardew, 1975; Lemaitre, 1976; Wu, 1978; Amestoy et al., 1979). Consequently, the only morphological parameter needed is the radius of the crack in the considered plane, since the shape of the initial circle is not altered during micro propagation. The crack geometry is taken into account by a dimensionless factor Y so that the energy release rate $\mathcal{G}$ is given by

$$E\mathcal{G} = Y^2\|\underline{\sigma}\|^2 a \tag{9}$$

where $\|\underline{\sigma}\|$ denotes an equivalent uniaxial stress (here the maximum principal stress σ_1), and E the Young's modulus of the virgin material. The values of the parameter Y depend upon the geometry of the initial flaw and on the fact that this flaw intersects or not a free surface. The crack propagation law is assumed to be described by an expression similar to that of Eq. (8) written in terms of the energy release rate $\mathcal{G}$ instead of the stress intensity factor K

$$\frac{da}{dt} = C(E\mathcal{G})^{n/2},\quad \mathcal{G}_{th} \leq \mathcal{G} \leq \mathcal{G}_c \tag{10}$$

and the parameters characterizing the crack propagation law are still C and n. Equation (10) is consistent with Eq. (8) in the case of pure mode I conditions.

Moreover, when the maximum principal stress σ_I is very large compared with the other two principal stresses σ_{II} and σ_{III}, the approximations made in this sub-section are not strong. The initial flaw size distribution to consider is denoted by $f_0(a)$. Because of the approximations made in this section, the general results derived in Section 2 can be simplified, and are studied in the following section by only considering the flaw size as a morphological parameter modeling the flaw distribution.

4 Simplified Reliability Analysis

In this Section, we assume that the flaw distribution is only dependent upon the size of the initial flaws and will be denoted by $f_0(a)$.

4.1 Expression for the Failure Probability. If the probability density function is assumed only to be dependent upon the flaw size, the failure probability, P_{F0}, of an RVE of volume V_0, is the probability of finding an initial flaw, whose size is larger than the critical flaw size. Rewriting Eq. (5) in the case of one parameter, the failure probability, P_{F0}, can be rewritten as (Hild and Roux, 1991)

$$P_{F0}(Q, \tau) = \int_{\psi[a_c(Q,\tau)]}^{+\infty} f_0(a)da \tag{11}$$

where $\psi(a_c)$ denotes the initial flaw size that, after a time τ, reaches the critical flaw size a_c obtained by integration of Eq. (9). It is referred to as *initial critical flaw size*. Its derivation is addressed in sub-Section 4.2. By means of Eq. (6), a simplified relationship between the initial flaw distribution and the failure probability of a structure Ω can be derived

$$P_F(Q, \tau) = 1 - \exp\left\{\frac{1}{V_0}\int_\Omega \ln\left(1 - \int_{\psi[a_c(Q,\tau)]}^{+\infty} f_0(a)da\right)dV\right\} \tag{12}$$

Equation (12) constitutes a unified expression for the failure probability with or without SCG. It relates the expression for the failure probability to the initial flaw size distribution f_0. In the next sub-section, expressions of the initial critical flaw size are derived.

4.2 Initial Critical Flaw Size. Expressions of the initial critical flaw size are derived under static (e.g. constant stress level) and dynamic conditions (e.g. linear stress level with time) by integration of Eq. (8)

$$\int_{\psi[a_c(Q,\tau)]}^{a_c(Q)} x^{-n/2}dx = \int_{t_I}^{t_F} CY^n\|\underline{\sigma}(Q, \tau)\|^n d\tau \tag{13}$$

where t_I denotes the initiation time ($Y^2\|\underline{\sigma}(Q(t_I), t_I)\|^2 a = E\mathcal{G}_{th}$) and t_F the failure time ($Y^2\|\underline{\sigma}(Q(t_F), t_F)\|^2 a = E\mathcal{G}_c$). These expressions enable to compute the failure probability of an RVE given in Eq. (11). In the following, σ_F denotes the value of the equivalent stress $\|\underline{\sigma}(Q(t_F), t_F)\|$ at failure. We define a scaling flaw size a_*, so that the scaling stress S_* corresponds to the failure stress of the scaling flaw: $Y^2 S_*^2 a_* = E\mathcal{G}_c$.

4.2.1 Static Conditions. Under static condition, the initiation time is equal to zero and integration of Eq. (13) shows that the normalized critical initial flaw size, $\psi(a_c)/a_*$ is related to the normalized failure stress σ_F/S_* and the time to failure under static condition t_{SF} by

$$\frac{\psi(a_c)}{a_*} = \left(\frac{S_*}{\sigma_F}\right)^2\left\{1 + \frac{n-2}{2}\left(\frac{\sigma_F}{S_*}\right)^2 \bar{t}_{SF}\right\}^{2/(2-n)}$$

$$\text{if}\quad \frac{\mathcal{G}_{th}}{\mathcal{G}_c} \leq \frac{\psi(a_c)}{a_*}\left(\frac{\sigma_F}{S_*}\right)^2 \leq 1 \tag{14}$$

with $\bar{t}_{SF} = CY^2(E\mathcal{G}_c)^{n/2-1}S_*^2 t_{SF}$.

4.2.2 Dynamic Conditions. When the stress evolution is linear with time, $\sigma = \dot{\sigma}t$, integration of Eq. (13) enables us to relate the normalized stress velocity $\dot{\sigma}/\dot{S}_*$ to the normalized failure stress σ_F/S_* by

$$\frac{2(n+1)}{(n-2)}\frac{\dot{\sigma}}{\dot{S}_*}\left(\frac{\sigma_F}{S_*}\right)^{-3} = \frac{\left(\dfrac{k}{\left\{\dfrac{\psi(a_c)}{a_*}\right\}^{1/2}\dfrac{\sigma_F}{S_*}}\right)^{n+1} - 1}{\left[1 - \left(\left\{\dfrac{\psi(a_c)}{a_*}\right\}^{1/2}\dfrac{\sigma_F}{S_*}\right)^{2-n}\right]} \tag{15}$$

with $\dot{S}_* = CY^2(E\mathcal{G}_c)^{n/2-1}S_*^3$, and $k = (\mathcal{G}_{th}/\mathcal{G}_c)^{1/2}$. The quantity $(\psi(a_c)/a_*)^{1/2}(\sigma_F/S_*)$ is bounded by k and 1. It is worth noting that when $Y\psi(a_c)^{1/2}\sigma_F$ approaches $(E\mathcal{G}_{th})^{1/2}$ the stress velocity $\dot{\sigma}$ approaches zero: this effect is due to the threshold energy release rate under which no SCG occurs. Conversely, when $Y\psi(a_c)^{1/2}\sigma_F$ approaches $(E\mathcal{G}_c)^{1/2}$ the stress velocity $\dot{\sigma}$ approaches infinity: there is no SCG phenomenon. Equation (15) constitutes an implicit relationship between the failure stress σ_F and the stress rate $\dot{\sigma}$. Figure 2 shows the evolution of the left-hand side of Eq. (15) as a function of normalized initial critical flaw size $(\psi(a_c)/a_*)^{1/2}(\sigma_F/S_*)$.

It is possible to relate the time to failure under static condition, t_{SF}, to the time to failure under dynamic condition, t_{DF}, and the time to initiation under dynamic conditions, t_{DI}, when the failure stress level is the same under static and dynamic conditions

$$t_{DF} = (n+1)t_{SF} + t_{DI}k^n\left(\frac{\psi(a_c)}{a_*}\right)^{-n/2}\left(\frac{\sigma_F}{S_*}\right)^{-n} \qquad (16)$$

In most practical cases, Eq. (16) can be simplified: the parameter n has often a value between 10 and 30. Since the value of the ratio k is on the order of 0.5, the term $k^n(\psi(a_c)/a_*)^{-n/2}(\sigma_F/S_*)^{-n}$ is often very small compared to unity. Therefore the normalized critical initial flaw size, $\psi(a_c)/a_*$ is related to the normalized failure stress σ_F/S_* and to the time to failure t_{DF} by

$$\frac{\psi(a_c)}{a_*} = \left(\frac{S_*}{\sigma_F}\right)^2\left\{1 + \frac{n-2}{2(n+1)}\left(\frac{\sigma_F}{S_*}\right)^2\bar{t}_{DF}\right\}^{2/(2-n)} \qquad (17)$$

with $\bar{t}_{DF} = CY^2(E\mathcal{G}_c)^{n/2-1}S_*^2t_{DF}$. The previous approximation is only valid when $(\psi(a_c)/a_*)(\sigma_F/S_*)^2$ is close to unity. In that case, the influence of the threshold energy release rate, $\mathcal{G}_{th}$ is negligible. When Eq. (17) is compared with Eq. (14), the well known relationship between the static life t_{DF} and the dynamic life t_{SF} is found: $t_{DF} = (n+1)t_{SF}$ (Davidge et al., 1973). On the other hand, when the ratio $(\psi(a_c)/a_*)(\sigma_F/S_*)^2$ is on the order of k, the previous approximation is not valid (Fig. 2). A series expansion about $(\psi(a_c)/a_*)(\sigma_F/S_*)^2 = k$ of Eq. (15) leads to the following result

$$\frac{\psi(a_c)}{a_*} \cong \left(\frac{kS_*}{\sigma_F}\right)^2 \times \left\{1 + \frac{1}{\dfrac{n-2}{2(k^{2-n}-1)}\left(\dfrac{\sigma_F}{S_*}\right)^2\bar{t}_{DF} + \dfrac{n-6+(n+2)k^{n-2}}{2(1-k^{n-2})}}\right\}^2 \qquad (18)$$

When $k^{n-2} \ll 1$, Eq. (18) can be rewritten as

$$\frac{\psi(a_c)}{a_*} \cong \left(\frac{kS_*}{\sigma_F}\right)^2\left\{1 + \frac{1}{\dfrac{n-2}{2k^{2-n}}\left(\dfrac{\sigma_F}{S_*}\right)^2\bar{t}_{DF} + \dfrac{n-6}{2}}\right\}^2 \qquad (19)$$

Figure 2 shows the two approximations about $(\psi(a_c)/a_*)(\sigma_F/S_*)^2 = k$ given by Eq. (18) and about $(\psi(a_c)/a_*)(\sigma_F/S_*)^2 = 1$ given by Eq. (17) compared with the exact solution given by Eq. (15). The approximation about $(\psi(a_c)/a_*)(\sigma_F/S_*)^2 = 1$ is valid in a very large interval, whereas the approximation about $(\psi(a_c)/a_*)(\sigma_F/S_*)^2 = k$ is valid only in a narrow interval.

4.3 Upper and Lower Bounds. By definition, Eq. (10) shows that $\psi(a_c)$ is greater than a_{th} (when $\mathcal{G} = \mathcal{G}_{th}$) and less than a_c (when $\mathcal{G} = \mathcal{G}_c$). This result can be extended to all initial flaws, i.e., to the initial flaw distribution, and two bounds can be obtained.

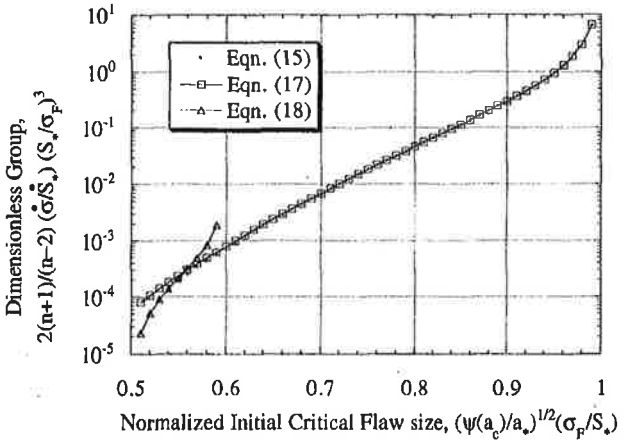

Fig. 2 Comparison of the evolution of a dimensionless group, $2(n+1)/(n-2)(\dot{\sigma}/\dot{S}_*)(S_*/\sigma_F)^3$, as a function of normalized initial critical flaw size, $(\psi(a_c)/a_*)^{1/2}(\sigma_F/S_*)$, by using Eqs. (15), (17), and (18). The parameter n is equal to 16, and the energy release rate ratio k is equal to 0.5.

In inert environment, i.e., when SCG does not occur, Eq. (11) holds with $\psi(a_c)$ equal to a_c. This particular case corresponds to an upper bound of the expression for the failure probability, denoted by $P_{F\text{-}UB}$

$$P_{F\text{-}UB}(Q) = 1 - \exp\left\{\frac{1}{V_0}\int_\Omega \ln\left(1 - \int_{a_c(Q)}^{+\infty} f_0(a)da\right)dV\right\} \qquad (20)$$

On the other hand, $\psi(a_c)$ may be substituted into a_{th} defined as the initial threshold flaw size obtained when $\mathcal{G} = \mathcal{G}_{th}$. This particular case corresponds to another bound, viz. a lower bound of the failure probability, denoted by $P_{F\text{-}LB}$

$$P_{F\text{-}LB}(Q) = 1 - \exp\left\{\frac{1}{V_0}\int_\Omega \ln\left(1 - \int_{a_{th}(Q)}^{+\infty} f_0(a)da\right)dV\right\} \qquad (21)$$

Equation (21) shows that a crucial material parameter is the threshold energy release rate, $\mathcal{G}_{th}$. This factor allows to derive an expression for a lower bound of the failure probability. A second crucial information is the flaw distribution. Because of linearity between external loads and stress field, and because $\mathcal{G}$ is a homogeneous function of degree 2 of the applied load Q, the following result applies

$$P_{F\text{-}LB}(kQ) = P_{F\text{-}UB}(Q) \qquad (22)$$

This result shows that for a given failure probability, the failure stress corresponding to the lower bound is equal to the failure stress corresponding to the upper bound times the ratio k.

5 Correlation to a Weibull Law

This section is devoted to the analysis of a particular flaw size distribution. We assume that the initial flaw size distribution is approximated by a power law function for very large flaw sizes

$$f_0(a) \cong \frac{\kappa}{a_*}\left(\frac{a}{a_*}\right)^{-p} \qquad (23)$$

where κ is a dimensionless constant. This function may correspond to the expression of a modified Gamma density function (Jayatilaka and Trustrum, 1977)

$$f_0(a) = \frac{1}{a_* \Gamma(p-1)} \left(\frac{a_*}{a}\right)^p \exp\left(-\frac{a_*}{a}\right) \qquad (24)$$

where Γ represents the Euler integral of the second kind. When the ratio a/a_* becomes large, the function f_0 is proportional to a power law function with $\kappa = 1/\Gamma(p-1)$.

By using the previous assumption it is possible to correlate the failure probability of a structure to a Weibull law. In this section we assume that an initial flaw is only described by a flaw size. The failure probability, P_{F0}, is assumed to be very small as compared to unity. The initial flaw size distribution can therefore be approximated by a power law function. When the ratio $(\psi(a_c)/a_*)(\sigma_F/S_*)^2$ is close to unity, the failure probability of a single link, P_{F0}, can be rewritten as

$$P_{F0} \cong \frac{\kappa}{p-1} \left(\frac{\sigma_F}{S_*}\right)^{2(p-1)} \left\{1 + \frac{n-2}{2} \left(\frac{\sigma_F}{S_*}\right)^2 \bar{t}_F\right\}^{[2(p-1)/(n-2)]} \qquad (25)$$

where $\bar{t}_F$ is either equal to $\bar{t}_{SF}$ or $\bar{t}_{DF}/(n+1)$. The failure probability of a structure, P_F, can then be rewritten as

$$P_F \cong 1 - \exp\left\{-\frac{1}{V_0}\int_\Omega P_{F0} dV\right\} \qquad (26)$$

When the term $(\sigma_F/S_*)^2\bar{t}_F$ is very small compared with unity, i.e., $\psi(a_c)/a_*(\sigma_F/S_*)^2 \cong 1$, the expression for the failure probability, P_F, becomes

$$P_F \cong 1 - \exp\left\{-\frac{1}{V_0}\int_\Omega \frac{\kappa}{p-1}\left(\frac{\sigma_F}{S_*}\right)^{2(p-1)} dV\right\} \qquad (27)$$

This expression is similar to a two-parameter Weibull law (Jayatilaka and Trustrum, 1977; Hild and Marquis, 1992). This case corresponds to fast fracture or fracture in an inert environment, and therefore gives an approximation of the upper bound of the failure probability given in Eq. (20). When the term $(\sigma_F/S_*)^2\bar{t}_F$ is very large compared to unity, i.e. $\psi(a_c)/a_*(\sigma_F/S_*)^2 \cong k$, the expression for the failure probability, P_F, can be rewritten as

$$P_F \cong 1 - \exp\left\{-\frac{1}{V_0}\int_\Omega \frac{\kappa}{p-1}\left(\frac{\sigma_F}{kS_*}\right)^{2(p-1)} dV\right\} \qquad (28)$$

This expression again is similar to a two-parameter Weibull law in which the scale parameter becomes kS_* instead of S_* in Eq. (27). This modification can also be seen as a change in critical conditions: instead of the failure criterion ($\mathcal{G} = \mathcal{G}_c$), one uses the initiation criterion ($\mathcal{G} = \mathcal{G}_{th}$). This case gives an approximation of the lower bound of the failure probability given in Eq. (21). The result shown in Eq. (22) is also found when Eq. (28) is compared to Eq. (27). Lastly, when the two previous approximations are not valid, there is a coupling between the stress level and the time to failure (see for instance Eq. (25)) and it is not possible *a priori* to correlate the failure probability to a Weibull law.

6 Analysis of Four-Point Flexure Tests

In the following, we analyze the experimental results carried out on a spinel Mn Zn ferrite. One hundred machined rectangular-type specimens (45 mm × 4 mm × 8 mm) were subjected to four-point flexure in air at room temperature. The inner span was equal to 20 mm and the outer span was equal to 40 mm. Five different stress rates were applied (0.0975, 9.75, 48.75, 487.5, and 9750 MPa/s). In this analysis, for the sake of simplicity, only the part of the material within the inner span length is considered. Verifications on the whole structure have shown that this hypothesis was not too restrictive. In four-point flexure, the stress field is considered mainly one-dimensional. From post-mortem analyses, initiation occured within the volume and therefore the approximations made in Section 3 are consistent with these observations.

The flaw size distribution is first determined by analysis of the experimental data at the lowest stress rate. The identification procedure can be decoupled if the lowest stress rate corresponds to the lower bound described in Eq. (21). The flaw size distribution $f_0(a)$ is assumed to be described by a Gamma density function

$$f_0(a) = \frac{1}{a_* \Gamma(p)} \left(\frac{a}{a_*}\right)^{p-1} \exp\left(-\frac{a}{a_*}\right) \qquad (29)$$

By using a least squares method, the following parameters are obtained: $p = 6.4$, $S_* = 160$ MPa, when $V/V_0 = 2400$ to fit the experimental results at the lowest stress rate. The values of the material parameters modeling SCG are then identified by using the experimental data at highest stress rate: $CY^2(E\mathcal{G}_c)^{n/2-1} = 3.2\,10^{-3}\,\mathrm{m^2\,MPa^2\,s^{-1}}$, $n = 20$, $k = 0.625$. In Fig. 3 the identified curve is plotted and compared with the experimental data for the highest and the lowest stress rates. The value of the parameter n is consistent with that found in double torsion experiments on a sharp crack ($n = 20$). If the material parameters previously obtained are used, it is found that the lower bound given in Eq. (21) coincides with the failure probability computed by using Eq. (12). This result shows that the hypothesis made *a priori* to identify the flaw size distribution as well the parameters of the crack growth law, is satisfied *a posteriori*. In the same figure, the failure probability corresponding to the upper bound is plotted. The experiments almost all lie between the lower bound and the upper bound. Furthermore, the predictions of the highest stress level are quite close to the predictions of the upper bound.

In Fig. 4 the three other stress rates are analyzed. The same material parameters are used. The predictions are in reasonable agreement with the experiments. All these results show that Eq. (12) is capable of modeling a series of experiments performed at very different stress rates. In particular, the expressions of the lower and upper bounds are consistent with the experimental observations. The discrepancy observed for the intermediate stress levels can be explained at least by two reasons. First, the crack growth law parameters are identified at the highest stress

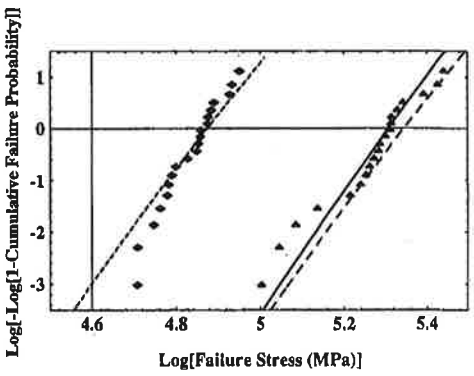

Fig. 3 Evolution of the failure probability, P_F, as a function of failure stress for a spinel Mn Zn ferrite subjected to dynamic fatigue in four-point flexure at two different stress rates (♦ = 0.0975 and ▲ = 9750 MPa/s), in air at room temperature. The solid line represents the identification at the highest stress level, and the dashed lines correspond to the identified upper and lower bounds.

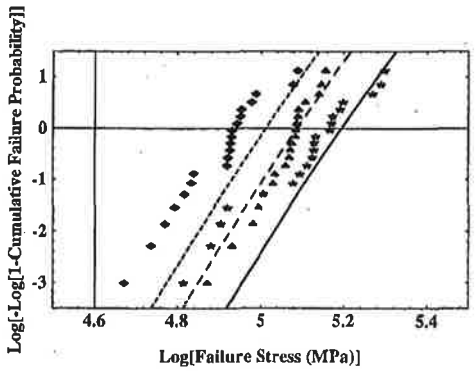

Fig. 4 Evolution of the failure probability, P_F, as a function of failure stress for a spinel Mn Zn ferrite subjected to dynamic fatigue in four-point flexure, in air at room temperature, at a stress rate equal to:

9.75 MPa/s (♦ = experiments, --- = identification),
48.75 MPa/s (▲ = experiments, – – = identification),
487.5 MPa/s (★ = experiments, —— = identification).

rate where the influence of the threshold is weak. Equation (10) overestimates the crack growth rate near the threshold energy release rate $\mathcal{G}_{th}$. The difficulty can be overcome by better accounting for the crack growth law near the threshold. Second, the flaw size distribution may vary from one set of specimens to another. This fact may explain the experimental observations for the first four failure probabilities when the stress rate is equal to 48.75 and 478.5 MPa/s. A post-inspection measuring the actual flaw size distributions could solve this problem.

7 Conclusion

An expression for the failure probability of a structure was derived in the framework of the weakest link theory and the independent events assumption. This expression models a brittle material subjected or not to Subcritical Crack Growth. The failure probability of a structure can be related to the initial flaw distribution through the evaluation of the set of initial critical flaws.

To assess the reliability of structures made of materials exhibiting Subcritical Crack Growth, one needs to devise a crack propagation law modeling the evolution and the possibility of crack kinking. Most of the data are obtained under pure mode I conditions, in which no kinking is involved. Under the assumption that all the flaws leading to the failure of a structure are initial sphere-like flaws, the crack propagation law is assumed to be similar to that in pure mode I condition. The consequence is that the only morphological parameter to consider is flaw size.

When the distribution is only a function of initial flaw size, a function ψ is used to find the initial critical flaw size: it depends upon the crack growth law that is used. Some simple results can be obtained at the level of a Representative Volume Element. Two bounds of the failure probability are obtained. The upper bound corresponds to the case where no Subcritical Crack Growth is involved. The failure conditions are then directly linked with a critical energy release rate. Conversely, the lower bound corresponds to initiation conditions related to a threshold energy release rate. These bounds can also be approximated by two different Weibull laws in which the shape parameters are the same, and the scale parameters are related by the energy release rate ratio.

Experiments on a spinel Mn Zn ferrite were performed at five different stress rates. The identifications of the parameters of the flaw size distribution give relatively good results by considering the highest and the lowest stress rates. The five sets of experiments show that Subcritical Crack Growth was involved at four stress rates. To avoid Subcritical Crack Growth the highest stress rate should have been at least one order of magnitude higher. On the other hand, the lowest stress rate coincides with the results given by the expression for a lower bound of the failure probability. This stress rate enables to get an information on the threshold energy release rate. The intermediate stress rates are relatively well described. These results show that the expression for the failure probability derived in this paper is able to account for Subcritical Crack Growth at low, medium and high stress rates. They also show that the expressions of an upper bound and a lower bound are consistent with experimental observations.

References

Amestoy, M., H. D. Bui, and K. Dang-Van, 1979, "Déviation infinitésimale d'une fissure dans une direction arbitraire," *C. R. Acad. Sci. Paris*, Vol. B t. 289, pp. 99–103.

Aoki, S., and M. Sakata, 1980, "Statistical Approach to Delayed Fracture of Brittle Materials," *Int. J. Fract.*, Vol. 16, pp. 459–469.

Aoki, S., I. Ohta, H. Ohnabe, and M. Sakata, 1983, "Statistical Approach to Time-Dependent Failure of Brittle Materials," *Int. J. Fract.*, Vol. 21, pp. 285–300.

Batdorf, S. B., and J. G. Crose, 1974, "A Statistical Theory for the Fracture of Brittle Structures Subjected to Polyaxial Stress States," ASME *Journal of Applied Mechanics*, Vol. 41, pp. 459–465.

Bilby, B. A., and G. E. Cardew, 1975, "The Crack with a Kinked Tip," *Int. J. Fract.*, Vol. 11, pp. 708–712.

Brinkman, C. R., and S. F. Duffy, 1994, "Life Prediction Methodologies and Data for Ceramic Materials (STP 1201)," ASTM, Philadelphia, PA.

Davidge, R. W., J. R. McLaren, and G. Tappin, 1973, "Strength-Probability-Time (SPT) Relationship in Ceramics," *J. Mat. Sci.*, Vol. 8, pp. 1699–1705.

Evans, A. G., 1972, "A Method for Evaluating the Time-Dependent Failure Characteristics of Brittle Materials—and its Application to Polycrystalline Alumina," *J. Mat. Sci.*, Vol. 7, pp. 1137–1146.

Evans, A. G., and S. M. Wiederhorn, 1974, "Crack Propagation and Failure Prediction in Silicon Nitride at Elavated Temperature," *J. Mat. Sci.*, Vol. 9, pp. 270–278.

Evans, A. G., 1978, "A General Approach for the Statistical Analysis of Multiaxial Fracture," *J. Am. Ceram. Soc.*, Vol. 61, pp. 302–308.

Freudenthal, A. M., 1968, *Statistical Approach to Brittle Fracture*, in Fracture (Liebowitz, H., ed.) Academic Press, Vol. 2 pp. 591–619.

Hild, F., and S. Roux, 1991, "Fatigue Initiation in Heterogeneous Brittle Materials," *Mech. Res. Comm.*, Vol. 18, pp. 409–414.

Hild, F., and D. Marquis, 1992, "A Statistical Approach to the Rupture of Brittle Materials," *Eur. J. Mech., A/Solids*, Vol. 11, pp. 753–765.

Hild, F., and D. Marquis, 1995, "Fiabilité de matériaux avec défauts en propagation stable," *C. R. Acad. Sci. Paris*, Vol. IIb t. 320, pp. 57–62.

Jayatilaka, A. D. S., and K. Trustrum, 1977, "Statistical Approach to Brittle Fracture," *J. Mat. Sci.*, Vol. 12, pp. 1426–1430.

Kadouch, O., 1993, "Rupture différée sous sollicitations mécaniques des ferrites spinelles NiZn et MnZn," PhD dissertation, École Nationale Supéricure des Mines de Paris.

Kingery, W. D., H. K. Bowen, and D. R. Uhlmann, 1976, *Introduction to Ceramics*, Wiley, NY.

Lamon, J., and A. G. Evans, 1983, "Statistical Analysis of Bending Strengths for Brittle Solids: a Multiaxial Fracture Problem," *J. Am. Ceram. Soc.*, Vol. 66, pp. 177–182.

Lamon, J., 1988, "Statistical Approaches to Failure for Ceramic Reliability Assement," *J. Am. Ceram. Soc.*, Vol. 71, pp. 106–112.

Lemaitre, J., 1976, "Extension de la notion de taux d'énergie de fissuration aux problèmes tridimensionnels et non linéaires," *C. R. Acad. Sci. Paris*, Vol. B t. 282, pp. 157–160.

Weibull, W., 1939, "A Statistical Theory of the Strength of Materials," Roy. Swed. Inst. Eng. Res., 151.

Wu, C.-H., 1978, "Fracture under Combined Loads by Maximum-Energy-Release-Rate Criterion," ASME *Journal of Applied Mechanics*, Vol. 45, pp. 553–558.